FUZZY-AIDED TRACTOGRAPHY PERFORMANCE ESTIMATION APPLIED TO BRAIN MAGNETIC RESONANCE IMAGING

L. M. San José Revuelta

Dep. of Signal Theory and Communications, University of Valladolid
Campus Miguel Delibes, 47011, Valladolid, Spain
phone: + (34) 983 423660, fax: + (34) 983 423667, email: lsanjose@tel.uva.es
web: www.lpi.tel.uva.es/∼luismi

ABSTRACT

In this paper, a recursive fuzzy inference system that can be applied to estimate the error probability of tracking algorithms used in medical image processing systems is proposed. Specifically, we are interested in the fiber bundles estimation process (*fiber tracking*) in diffusion tensor (DT) fields acquired via magnetic resonance imaging (MRI). As tracking algorithm we consider a previously developed probabilistic tracking algorithm (PTA). This paper studies the analogies between this tracking approach and a typical Multiple Hypotheses Tracing (MHT) system, which is closely related to fuzzy systems. This comparison leads to the development of a SAM (Standard Additive Model) fuzzy system that on-line provides the uncertainty of the decisions about the estimated fiber tracts. Experiments on both simulated and real DT-MR images demonstrate the validity of the method.

1. INTRODUCTION

Diffusion Tensor (DT) Magnetic Resonance Imaging (MRI) has recently gained significant popularity due to its ability to measure the anisotropic diffusion of water in structured biological tissues [1]. Since in cerebral white matter most random motion of water molecules are restricted by axonal membranes and myelin sheets, diffusion anisotropy allows depiction of directional anisotropy within neural fiber structures.

The estimation of white matter fiber tracts in the brain –e.g. corpus callosum, corticospinal tract– becomes very interesting in many clinical applications: surgical planning, radiation therapy planning and 3-D visualization. Besides, strong demands exist to accomplish this task automatically by computer.

The DT is normally interpreted by calculating its eigenvalues and eigenvectors. That eigenvector corresponding to the largest eigenvalue describes the principal diffusion direction while the corresponding eigenvalue is a quantitative measure of the diffusion in that specific direction. Most of the existing methods for fiber tracking rely only on the direction of principal diffusion to create integral curves that estimate the fiber paths [2, 3]. Other approaches explore more of the information contained in the diffusion tensor. For example, Hagmann et al. [4], consider the tensor as a probability distribution. Parker et al. (2001) [5] and Campbell et al. [6] have proposed the use of level set theory to find the tracts. These approaches focus on the problem of preventing leakage from the bundle structure that represents the fibers. On the other hand, Batchelor [7] uses more of the tensor information by iteratively solving the diffusion equation. This way, paths are created that originate from a chosen seed-point and can be considered as probability measures of a tract. A similar approach is presented by O'Donnell et al. [8], where the steady state of the diffusion equation to create a flux vector field is found. The authors show how the inverse diffusion tensor can define a Riemannian metric that is used to find geodesic paths that can be interpreted as fiber tracts.

However, and due to both some deficiencies in these tracking algorithms and the corrupted data that is present in existing DT acquisitions (mainly due to noise, inhomogeneity or partial volume effect), tracking algorithms may depict fiber tracts which do not exist in reality or miss to visualize important branching structures. In order to avoid misinterpretations, the viewer of the visualizations must be provided with some information on the uncertainty of a depicted fiber and of its presence in a certain location. In this paper we will use a recently developed probabilistic tracking algorithm [9] that takes into account the whole information provided by the diffusion matrix, i.e., it does not only consider the principal eigenvector direction but the complete 3D information. Besides, the algorithm includes a procedure that adapts the number of *offspring paths* emerging from any studied voxel to the degree of anisotropy observed in its proximity, improving, this way, the estimation robustness in areas where multiple fibers cross while keeping complexity to a moderate level.

A parallelism between the proposed PTA and the MHT strategy [11, 12] is developed. Since the MHT procedure is directly related to fuzzy logic, a fuzzy inference engine for the estimation of the uncertainty of the tractography process will be then obtained. This recursive fuzzy system will calculate more reliable estimates of the tracts certainty. In Section 2, the main notions of the proposed tracking scheme are summarized, while Section 3 describes the basic concepts of the MHT approach, in order to establish a parallelism of concepts in both approaches. Next, in section 4, the development of a recursive SAM fuzzy system for the performance evaluation of the tracking scheme is studied. The paper finishes with the Numerical Results and the Conclusions sections.

For the sake of brevity, the reader interested in the review of previous related approaches can consult the corresponding section in [9].

2. PROBABILISTIC FIBER TRACKING ALGORITHM

The tracking algorithm used in this paper was initially developed in [9]. Thus, this section presents a summary of the method. The algorithm uses probabilistic criteria and iterates over several points in the analyzed volume (the points given by the highest probabilities in the previous iteration). The

algorithm starts in a user-selected seed voxel, V_0.

At every iteration, the method evaluates a set of parameters related to the central voxel of a $3 \times 3 \times 3$ cubic structure. The central point, V_c, represents the last point of the tract being analyzed. In the first iteration, $V_c = V_0$. There exist 26 possible directions to take for the next iteration (in order to select the next point of the tract).

2.1 Basic concepts

Once a DT-MR volume has been scanned, the tracking process starts in a user-selected seed voxel, V_0. A new point V_k is added to the estimated tract (or path) at every iteration of the algorithm. Point V_k is the voxel with the highest local probability P_l, a parameter which is calculated for every voxel that surrounds the last estimated point of the path.

Local probability P_l is calculated as

$$P_l = b(\xi_1 sp_1 + \xi_2 sp_2 + \xi_3 sp_3 + \xi_4 sp_4) + (1-b)P_l' \qquad (1)$$

where b stands for a weighting factor and ξ_1, ξ_2, ξ_3 and ξ_4 are the corresponding weights of the so-called *smoothness parameters*, sp_i (described in [13]). Both their mathematical expressions and their geometrical meaning are explained in [9]. These parameters measure the angles between the directions that join successive path points, as well as the angles between these directions and the eigenvectors associated to the largest eigenvalues found in those voxels. sp_2, sp_3 and sp_4 are used to maintain the local directional coherence of the estimated tract and avoid the trajectory to follow unlikely pathways. The threshold for sp_1 is set such that the tracking direction could be moved forward consistently and smoothly, preventing the computed path from sharp transitions.

2.2 Fractional anisotropy

Parameter P_l' in Eq. (1) can be written as

$$P_l' = \alpha \cdot \mu_1 \cdot fa(V_l) + (1-\alpha) \cdot \mu_2 \cdot P_l, \qquad 0 < \alpha < 1 \qquad (2)$$

where parameter α allows the user to give a higher relative weight to either the anisotropy or the local probability, and μ_1 and μ_2 are scaling factors. fa represents the fractional anisotropy, which is calculated as[1],

$$fa = \sqrt{\frac{(\lambda_1-\lambda_2)^2 + (\lambda_2-\lambda_3)^2 + (\lambda_1-\lambda_3)^2}{2(\lambda_1^2+\lambda_2^2+\lambda_3^2)}}, \qquad (3)$$

with $(\lambda_1, \lambda_2, \lambda_3)$ being the three eigenvalues of the diffusion matrix of voxel V_l. Finally, parameter P_l in Eq. (2) is calculated based on the probability of going from the last estimated voxel of the tract, V_c, to its surrounding voxels. This probability takes into account the eigenvalues and eigenvectors available at point V_c from the DT-MR image diffusion matrix. Specifically, it takes into account the projection of each of the eigenvectors to each of the directions involved in the change of spatial position from V_c to V_l.

Probabilities P_l in Eq. (1) can be recursively accumulated, yielding the probability of the path generated by the successive values of V_c,

$$P_{\text{path}}(k) = P_l^* \cdot P_{\text{path}}(k-1) \qquad (4)$$

[1]Though not explicitly shown, the set of values P_l' is properly normalized so that they can be interpreted as probabilities.

with k being the iteration number, $P_l^* = P_l / \sum_l P_l$, and $P_{\text{path}}(0) = 1$. At the end of the visualization stage, every estimated path is plotted with a color that depends on P_p.

2.3 Pool of possible seeds

At the end of each iteration, a pool of voxels is formed by selecting the s best voxels according to Eq. (1). The first voxel of the pool becomes the central voxel V_c at next iteration, expanding, this way, the current pathway. As proposed in [14], the value of s is adjusted depending on the degree of anisotropy found in current voxel V_c and its surroundings. When this anisotropy is high, it means that a high directionality exists in that zone, and the probability that V_c belongs to a region where fibers cross is really low. Consequently, s takes a small value (1, 2 or 3). On the other hand, if V_c is found to be situated in a region of high anisotropy, the probabilities of having fibers crossing or branching is higher. In this case, it is interesting to explore various paths starting in V_c. This can be achieved by increasing parameter s.

Notice that parameters $(a, b, \mu_1, \mu_2, \xi_1, \xi_2, \xi_3, \xi_4)$ must be adjusted in order to get satisfactory results when estimating the tracts of the volume being analyzed. This is a tedious task that has always been heuristically approached. In this paper, we have used the strategy proposed in [15], where a neural network with a variable number of hidden layers and the backpropagation algorithm for weights' learning is proposed for the estimation of these parameters. This adjustment is useful when the algorithm is applied to a different part of the brain (fiber bundles) or when the scanning conditions have changed.

3. PARALLELISM PTA *VS* MHT

A fuzzy version of Reid's classical MHT algorithm [12] was proposed in [11]. This system is based on the likelihood discrimination and it was applied to the tracking of natural language text-based messages. [11] shows the possibility of handling information about any time-varying phenomenon, as long as the phenomenon can be described by means of a few keywords, and the phenomenon itself is statistically causal in the sense that the distribution of future states is statistically dependent on the past observed states. This study has already been carried out through the mathematical analysis of *single-fuzzy-input single-fuzzy-output* feedback systems for hypotheses likelihood determination.

It is easy to see the following parallelism that leads to the possibility of a tract probability estimation based on text-messages (fuzzy-messages): (i) the natural-language messages in [11] and the noisy DT-MR image constitute, in both cases, the source of *noisy* or *ambiguous* information, (ii) the *tracks* used in the MHT algorithm, which are defined as *sequences of associated symbols*, can be clearly associated to the possible sequences of points in the 3D space, in the tracking context, (iii) the system in [11] associates multiple messages generated along time by using a specific stochastic model for the applications' dynamics. In our case, this model can be the information provided by the anisotropy measured using Eq. (3), (iv) the term *target* denotes some condition that generates observable phenomena. In our context, these targets are the sequences of points that define a tract.

Another important issue that must be taken into account is that the fuzzy inference rules that update the

tracks/sequences probabilities (Fig. 3 in [11]) must now be especially adapted. In our problem, every time a new point V_k is processed, the set of possible tract hypotheses is increased, with equiprobable hypotheses.

As a consequence, the MHT system can be viewed as a probabilistic approach for multiple targets tracking. Theoretically, this algorithm conserves *all* the hypotheses that explain the observation until certain time, together with an estimation of the probability of each hypothesis [11]. At the end, the hypothesis with the highest likelihood is taken as the solution. On the other hand, the uncertainty in the prediction of the future positions found in the MHT of [11], resembles the creation of new fiber tracts based on the previous ones. The PTA maintains a finite set of hypotheses (see the *pool of future seeds* in section 2.1) with their associated probabilities, and tracts are visualized based on these data.

4. FUZZY ESTIMATION OF TRACTOGRAPHY PERFORMANCE

In this section we propose a recursive SAM (Standard Additive Model [16]) fuzzy subsystem that allows to monitor the performance of a DT-MRI tracking system such as our PTA. The SAM model allows to work with linguistic descriptions and ambiguities. This kind of description allows to fuzzy-quantify the errors in the tractography problem.

The system here proposed consists in three connected fuzzy inference engines (FIEs), as depicted in Fig. 1. It is necessary to develop an algorithm where the inputs to the MHT system have some correlation.

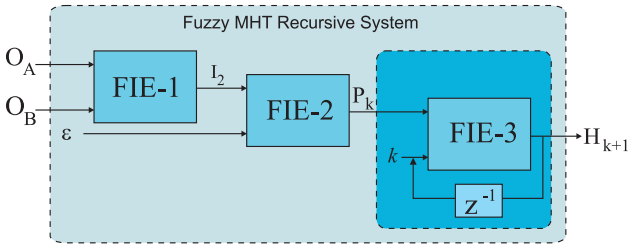

Figure 1: Recursive SAM fuzzy system for estimation of the error probability of the estimated error tracts.

The inputs O_A and O_B to FIE-1 are two different tracts (hypotheses) estimated by the algorithm sharing in common the first and the last points (in practice, both tracts must start and finish in near voxels). These tracts are prolonged on one side with a new sample every time a new point is considered (at every iteration of the tracking algorithm), while the last point of the tracts is lost. This way, the compared tracts have always the same length.

In order to evaluate the similarity between two tract hypotheses O_A and O_B, it is necessary to quantify their similarity using a 3D distance. As a consequence, a *similarity coefficient* that depends on the distance between these two considered tracts can be assigned.

In order to implement a fuzzy system, we must establish a relation between this *crisp* value (defined in $[0-M]$) and the fuzzy sets where a linguistic variable is defined. This relation is shown is Fig. 2.

This allows to obtain the possible fuzzy values of I_2 (output of the first FIE and input to the second).

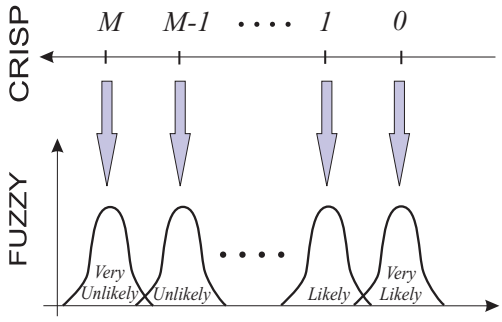

Figure 2: Fuzzification of the crisp similarity between tract hypotheses O_A and O_B.

Next, we relate the *prediction error* ε used as input in the FIE-2 with the anisotropy observed in the last (currently processed) point of the tract. This way, if a large anisotropy is obtained, the tract would be rather smooth in the proximity of the current voxel and ε will take a small value for those hypotheses (future points to expand the current tract) that involve a small change in the fiber direction. On the other hand, when the anisotropy is small (meaning an isotropic volume area), parameter ε would be the same for every direction (hypotheses). The value of ε must, also, be fuzzified.

This way, the FIE-1 estimates the likelihood of two close tracts. Next, FIE-2 weights this estimate with respect to the prediction error (that is inversely proportional to the anisotropy) and obtains a second likelihood. This value is used to update the *global likelihood* (or *global reliability*), which is a measure of the tracking estimation error probability. This third process is performed by FIE-3. Thus, this third block updates, with a feedback system, the previous system knowledge every time a new point is processed.

5. NUMERICAL RESULTS

In order to evaluate the proposed algorithm, we have used both synthetic and real DT-MR images.

5.1 Synthetic images

First, four different synthetic DT-MRI data in a $50 \times 50 \times 50$ grid have been generated (see Fig. 3). The first three images were used for testing in [9]. To make the simulated field more realistic, Rician noise [17] was added to the diffusion weighted images which were calculated from the Stejskal-Tanner diffusion equation[2] using the gradient sequence in [18] and a *b*-value of 1000.

The noisy synthetic diffusion tensor data was obtained using an analytic solution to the Stejskal-Tanner equation. Eigenvectors in the isotropic areas were: $\lambda_1 = \lambda_2 = \lambda_3$, while in the remaining voxels of the image $\lambda_1 = 7$, $\lambda_2 = 2$, $\lambda_3 = 1$. In our study, the SNR varies from 5 to 30 dB.

The "star" image consists of six orthogonal sine half-waves, each of them with arbitrary radius. This is the most complicated situation since the diffusion field experiments variations with the three coordinate axes and there exists a crossing region. Three different tracking results are shown in Fig. 3 bottom-right. Estimated tracts are printed over the

[2]This equation relates diffusion weighted measurements (S) to measurements without diffusion weighting (S_0): $S = S_0 \exp(-dD)$, with D being the diffusion coefficient.

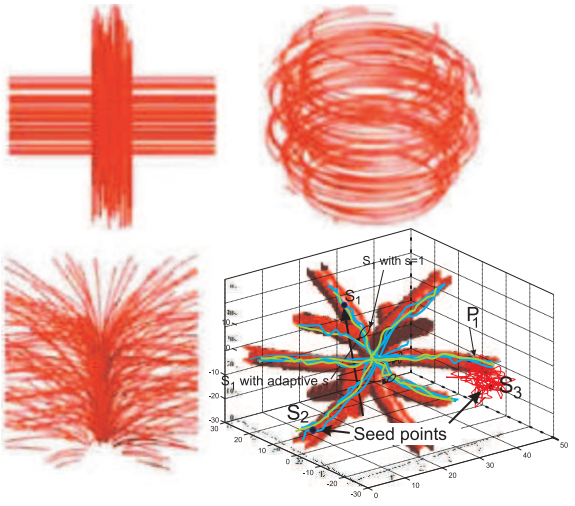

Figure 3: Synthetic DT-MR images used for testing the proposed algorithm: “cross” (top, left), “earth”, “log” and “star” (bottom, right).

red synthetic image. The algorithm is always able to follow the right paths. (Tracking examples for the other simpler synthetic images can be found in [9]).

The differentiation between voxels belonging to a fiber or to a very isotropic area, respectively, is attained by mapping the path probabilities given by the output of the FIE-3 (see Fig. 1) into a color scale and classifying them according to some fixed thresholds[3]. Three different seeds (S_1, S_2 and S_3) are shown on the star figure. S_1 and S_2 belong to the intrinsic volume (voxels with a very high anisotropy) and the algorithm moves through the most probable direction following the main direction of the cross in each situation. On the other hand, when an extrinsic point such as S_3 is selected as seed, the algorithm explores in the neighboring voxels until it finds a voxel with a high anisotropy value (point P_1). Once P_1 is found, the tracking algorithm proceeds as in the case of S_1 and S_2.

These simulations show how the algorithm finds the proper fiber path whatever (extrinsic or intrinsic) seed voxel is chosen. Notice that, the extrinsic seeds S_3 are located far away from the fiber bundles region, thus making the algorithm explore a wider range of points before reaching the points P_1 that belong to an existing fiber path.

Next, we compare the estimates of the tracts certainty of the probabilistic tracking algorithm (PTA) described in section 2.1 with and without implementing the fuzzy engine for estimating the probability of error. Figure 4 shows the mean probability of wrong estimation (average value in 10 executions) and Fig. 5 presents the mean variance of these estimators, for different signal qualities.

It can be seen that: (i) the probability of error increases as the SNR of the original image improves; more complex images have larger tracking error estimates, (ii) the tracking error improves notably when the fuzzy engine is used for estimation, and (iii) though not shown in the Figure, the fuzzy engine was also added to a Bayesian tracking approach similar to that proposed in [10]. Analyzing this case, it could be appreciated that the PTA-fuzzy algorithm obtained slightly

[3]If no fuzzy system is used, the path probabilities are given by Eq. (4).

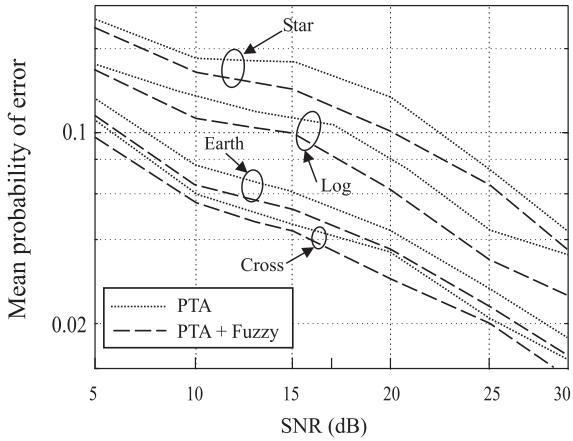

Figure 4: Mean probability of error of the probabilistic tracking scheme proposed, with and without the fuzzy method for estimation of the probability of error. Synthetic images from Fig. 3 were used.

more accurate certainty estimates.

Figure 5 shows how the fuzzy procedure greatly decreases the variance of the estimator, leading to more robust and accurate estimations, specially for low quality images.

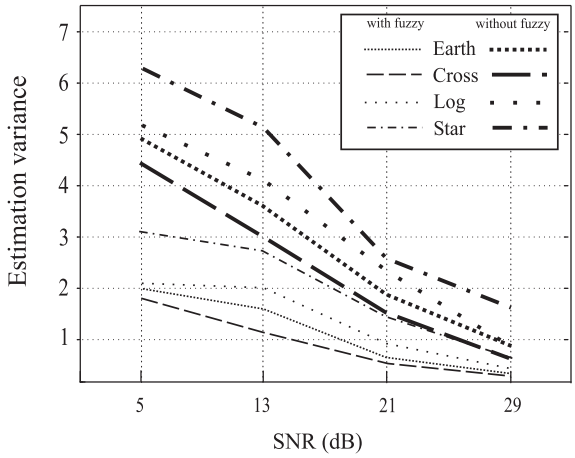

Figure 5: Variance of the reliability estimators for the four synthetic images. Bold traces correspond to PTA without fuzzy assistance. Non-bold lines correspond to PTA+fuzzy.

It can be observed that the fuzzy-aided approach gets much smaller estimation variances. This estimation procedure is rarely influenced by both the SNR of the image and image complexity (in terms of anisotropy).

5.2 Testing with real brain’s corpus callosum images

The proposed PTA is finally applied to a real DT-MR image. Specifically, we have selected the *corpus callosum* of the brain (see Fig. 6).

Tracking results are shown for six different trials. It can be appreciated how the algorithm is able to follow the main fiber bundle direction without getting out of the area of interest. As an example, we have included the second case (on the top-middle) were a wrong path arises from the correct fiber bundle.

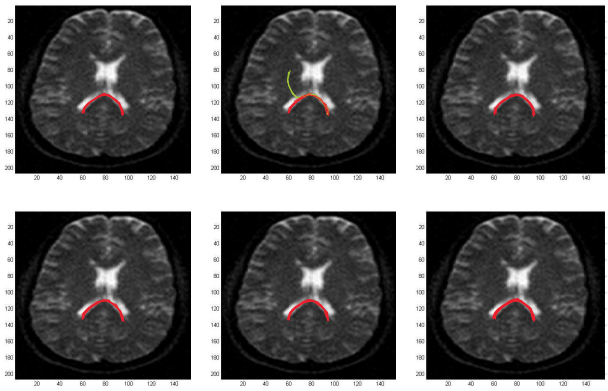

Figure 6: Different fiber bundles estimation results for the *corpus callosum* of the human brain.

When the variance of both certainty estimation methods (PTA and PAT+fuzzy) were calculated, we obtained values of 7.5 and 3.2, respectively. Thus, a direct consequence of the fuzzy aided system is that the variance of the estimation is reduced by approximately 50%.

6. CONCLUSIONS

A fuzzy inference algorithm that can be applied to estimate the certainty of different tracking schemes for DT-MR images has been developed and tested. The fuzzy engine was first derived from the text-based MHT strategy since fuzzy systems are closely connected to the MHT approach. A previously developed probabilistic tracking algorithm has been used to evaluate this fuzzy procedure [9]. Numerical simulations have been performed using both synthetic and real DT-MR images. In both cases, the certainty about the performance reliability was increased when the fuzzy system is used, providing, this way, more precise estimates of the probability of neuronal fiber connections.

7. ACKNOWLEDGEMENTS

The author acknowledges the Spanish CICYT for research grant TEC2007-67063/TCM.

REFERENCES

[1] S. P. Awate, H. Zhang, J. C. Gee, "A fuzzy, nonparametric segmentation framework for DTI and MRI analysis: with applications to DTI-tract extraction," *IEEE Transactions on Medical Imaging*, vol. 26, pp. 1525–1536, 2007.

[2] T. Conturo et. al., "Tracking neuronal fiber pathways in the living human brain," *Proc. Natl. Acad. Sci. USA*, vol. 96, pp. 10422–10427, 1999.

[3] B. Vemuri et al., "Fiber tract mapping from diffusion tensor MRI," in *P*roc. IEEE Workshop on Variational and Level Set Methods in Computer Vision, pp. 81–88, 2001.

[4] P. Hagmann et al., "DTI mapping of human brain connectivity: Statistical fibre tracking and virtual dissection," *NeuroImage*, vol. 19, pp. 545–554, 2003.

[5] G. Parker, C. Wheeler-Kingshott, G. Barker, " Distributed anatomical brain connectivity derived from diffusion tensor imaging," in *P*roc. IPMI, pp. 106–120, 2001.

[6] J.S.W. Campbell, K. Siddiqi, B.C. Vemuri, G.B. Pike, "A geometric flow for white matter fibre tract reconstruction," in *P*roc. Int. Symp. Biomed. Imag., 2002.

[7] P. Batchelor, F. Hill, F. Calamante, D. Atkinson, "Study of connectivity in the brain using the full diffusion tensor from MRI," in *P*roc. IPMI, pp. 121–133, 2001.

[8] L. O'Donnell et al., "New approaches to estimation of white matter connectivity in diffusion tensor MRI: elliptic pdes and geodesics in a tensor-warped space," in *P*roc. MICCAI 2002, 2002.

[9] L. M. San-José-Revuelta, M. Martín-Fernández, C. Alberola-López, "A new method for fiber tractography in diffusion tensor magnetic resonance images," in *Proc. ICSIP 2006*, Vol. I, Karnataka, India, December 7-9. 2006, pp. 380–385.

[10] O. Friman, C.-F. Westin, "Uncertainty in white matter fiber tractography," in *Proc. MICCAI 2005*, LNCS 3749, pp. 107–114, 2005.

[11] C. Alberola, G.V. Cybenko, "Tracking with text-based messages" *IEEE Intell. Systems*, vol. 14, pp. 70–78, 1999.

[12] D.B. Reid, "An algorithm for tracking nmultiple targets," *IEEE Tr. Automat. Contr.*, vol. AC-24, pp. 843–854, 1979.

[13] N. Kang, J. Zhang, E. S. Carlson, D. Gembris, "White matter fiber tractography via anisotropic diffusion simulation in the human brain," *IEEE Transactions on Medical Imaging*, vol. 24, pp. 1127–1137, 2005.

[14] L. M. San-José-Revuelta, M. Martín-Fernández, C. Alberola-López, "A new proposal for 3D fiber tracking in synthetic diffusion tensor magnetic resonance images," in *Proc. ISSPA 2007*, Sharjah, United Arab Emirates, February 12-15. 2007.

[15] L. M. San-José-Revuelta, "Improvement of DT-MRI processing algorithms using neural networks," in *Proc. MLSP 2007*, Thessaloniki, Greece, August 27-29. 2007, pp. 229–234.

[16] B. Kosko, *Fuzzy Engineering*, New Jersey: Prentice Hall Int'l, 1992.

[17] H. Gudbjartsson, S. Patz, "The Rician distribution of noisy MRI data," *Magnetic Resonance in Medicine*, vol. 34, pp. 910–914, 1995.

[18] C.-F. Westin et al., "Processing and visualization for DT-MRI," *Med. Image Analysis*, 6, pp. 93–108, 2002.